PREDICTING SECONDARY SOIL FERTILITY ATTRIBUTES USING XRF SENSOR WITH REDUCED SCANNING TIME IN SAMPLES WITH DIFFERENT MOISTURE CONTENT

Tiago Rodrigues Tavares [a,b*], José Paulo Molin [b], Thainara Rebelo da Silva [c], Hudson Wallace Pereira de Carvalho [a]

[a] Laboratory of Nuclear Instrumentation (LIN), Center for Nuclear Energy in Agriculture (CENA), University of São Paulo (USP), Piracicaba, São Paulo 13416000, Brazil;
[b] Laboratory of Precision Agriculture (LAP), Department of Biosystems Engineering, "Luiz de Queiroz" College of Agriculture (ESALQ), University of São Paulo (USP), 13418900 Piracicaba, São Paulo, Brazil;
[c] Laboratory of Agricultural Machinery and Precision Agriculture (LAMAP), Department of Biosystems Engineering, Faculty of Animal Science and Food Engineering (FZEA), University of São Paulo (USP), 13635900 Pirassununga, São Paulo, Brazil;

[*] Corresponding author: tiagosrt@usp.br

A paper from the Proceedings of the
15th International Conference on Precision Agriculture
June 26-29, 2022
Minneapolis, Minnesota, United States

Abstract.

To support future in situ/on-the-go applications using X-ray fluorescence (XRF) sensors for soil mapping, this study aimed at evaluating the XRF performance for predicting organic matter (OM), base saturation (V), and exchangeable (ex-) Mg, using a reduced analysis time (e.g., 4 s) in soil samples with different moisture contents. These attributes are considered secondary for XRF prediction because they do not present emission lines in the XRF spectrum. Ninety-nine soil samples acquired in two Brazilian agricultural fields were used. Soil samples with moisture content of 0, 5, 10, 15, 20, and 25 wt.% were measured by XRF under 4 s of dwell time. The results revealed that, despite the short dwell time, it was possible to obtain satisfactory predictions [residual prediction deviation (RPD) > 1.40] of V and ex-Mg in soil samples with up to 15 wt.% of moisture content. Satisfactory predictions of V were also possible with 20 and 25 wt.% of moisture content. Conversely, satisfactory predictions of OM were only possible in dried samples, yielding RPD of 1.60. Notwithstanding these promising results, for all studied attributes, the predictive performance gradually decreased as a function of water content in the soil. Nevertheless, we emphasize that the previously mentioned performance was obtained without the application of methods to mitigate the effect of moisture in spectral data [e.g., external parameter orthogonalization (EPO)]. Thus, methods to correct external effects on XRF data may lead to

The authors are solely responsible for the content of this paper, which is not a refereed publication. Citation of this work should state that it is from the Proceedings of the 15th International Conference on Precision Agriculture. EXAMPLE: Tavares, T. R.; Molin, J. P.; Silva, T. R. & Carvalho, H. W. P. (2022). Predicting secondary soil fertility attributes using XRF sensor with reduced scanning time in samples with different moisture content. In Proceedings of the 15th International Conference on Precision Agriculture (unpaginated, online). Monticello, IL: International Society of Precision Agriculture.

more accurate results, which highlights the necessity of further research to find the best method for mitigating the effect of soil moisture content in XRF spectra. This study emphasizes the potential of XRF for soil mapping in in situ analysis, being pioneering in showing that with a reduced scanning time it is possible to obtain satisfactory prediction performances for OM, V, and ex-Mg in wet samples.

Keywords.
1. X-ray fluorescence 2. On-the-go applications 3. Rapid soil analysis 4. Variable-rate applications

Introduction

The search for a fast, versatile and accurate method for soil fertility analysis is a prominent topic within precision agriculture since its conception (Khosla & Alley, 1999). Several sensing techniques have been proposed and tested for practical soil fertility assessments in order to increase the spatial density of analysis, e.g., apparent electrical conductivity sensors, diffuse reflectance spectroscopy in the visible and infrared (vis-NIR) sensors, among others (Viscarra Rossel et al., 2011).

The application of X-ray fluorescence (XRF) sensors for soil fertility analysis has evolved rapidly in recent years (Lima et al., 2019; Nawar et al., 2019; Tavares et al., 2020). The technique characterizes a wide range of soil elemental composition (*e.g.*, Ti, Fe, Cu, Ca, K, Si, among others), providing complementary information to other more common proximal soil sensing (PSS) techniques, such as mineralogical and organic constituents offered by visible and near infrared diffuse reflectance spectroscopy (VNIR) (O'Rourke et al., 2016). The characterization of the chemical elements present in the sample provided by XRF allows, in some cases, the inference of properties without direct spectral responses (e.g., pH, organic matter (OM), base saturation (V), and exchangeable (ex-) Mg) (Weindorf & Chakraborty, 2020), i.e., designated as secondary soil properties.

XRF sensors have the potential to evolve towards applications directly in the field, since their outputs are less affected by soil moisture than techniques traditionally applied *in situ* (e.g., vis-NIR sensors), and it is also quite flexible regarding sample preparation (Tavares et al., 2019). Although some studies have already reported applications of XRF directly in the field for soil evaluation (Weindorf et al., 2012; Stockmann et al., 2016), the scanning time typically used in these applications is around 30 to 90 s, which is quite contrasting when compared to the analysis time of other PSS techniques. For example, both apparent electrical conductivity (ECa) and vis-NIR techniques have an almost instantaneous scanning time (one second per scanning) that allows on-the-go data acquisitions with high spatial density (*e.g.*, 250 data points ha^{-1} at operating speeds around 4 m s^{-1}) (Molin & Tavares et al., 2019). An example closer to what would be realized for on-the-go application using XRF is the ion-selective electrodes (ISE) used in mobile platforms, since the ISE needs a longer dwell time in contact with the sample to stabilize its reading (*e.g.*, approximately 10 to 15 s) (Adamchuk et al., 2007). However, to the best of our knowledge, no work has explored XRF scanning times below 30 s for soil fertility analysis.

Another challenge of *in situ* analysis using soils sensors is to minimize the soil moisture effect that compromise part of the sensors' performance (Ge et al., 2005; Kuang and Mouazen, 2013). Strategies for calibrating of predictive models that are insensitive to the effect of soil moisture has received a great attention for *in situ* analysis performed with vis-NIR sensors (Minasny et al., 2011; Kuang and Mouazen et al., 2013; Nawar et al., 2020). However, there is still a lack of information on the soil moisture effect in XRF data, especially for data collected with reduced scanning time. In this context, to support future *in situ*/on-the-go applications using XRF sensors, the present study aimed at evaluating the trade-off among the XRF's performance and the increment of soil moisture in soil fertility predictions. In addition, this evaluation was performed using a reduced scanning time, simulating a possible scenario of on-the-go data acquisition.

Material and Methods

Soil samples

The samples used in this study belong to the soil sample bank of the Precision Agriculture Laboratory (LAP) from Luiz de Queiroz College of Agriculture, University of São Paulo. They were collected from 0–20 cm depth and stored after being air-dried, ground and sieved (≤ 2 mm). The samples used in this work are from two different fields that have been under active agricultural production. Field 1 is located in the Southeast Region of Brazil, in the municipality of Piracicaba, State of São Paulo. Its soil is classified as Lixisol with a clayey texture and high nutrient variability. Field 2 is situated in Brazil's Midwest Region, in the municipality of Campo Novo do Parecis, State of Mato Grosso. Its soil is classified as Ferralsol, with a texture varying between sandy loam and sandy clay loam. A set of 101 soil samples were selected for the present study, being 57 soil samples from Field 1 and 44 from Field 2. The chemical analysis results of the LAP's soil sample bank were used to choose samples with wide ranges of variability of key fertility attributes in both study fields. After dataset selection, the samples were again subjected to laboratory analyses, as described below, which provided the results of the reference analyses used in this work.

Reference analyses

From each sample, an aliquot of 90 g was sent to the laboratory for regular soil fertility tests. OM concentration was determined via oxidation with potassium dichromate solution. Extractable nutrients were determined via ion exchange resin extraction. The soil potential acidity (H + Al) was quantified via pH in buffer solution method (SMP) and used to calculate the cation exchange capacity (CEC), which corresponds to the sum of soil potential acidity and sum of bases (ex-Ca + ex-Mg + ex-K). V was calculated by the ratio between the sum of bases and CEC.

XRF measurements with reduced scanning time

A portable device Tracer III-SD model (Bruker AXS, Madison, EUA) was used for XRF data acquisition. This instrument has a 4 W Rh X-ray tube and a Peltier-cooled Silicon Drift Detector with 2048 channels. The X-ray tube was configured for voltage and current of 35 kV and 7 μA, respectively (Tavares et al., 2020). No filter was used and the measurements performed under atmospheric pressure. A scanning time of just 4 s was applied in this study. Three readings were taken from each soil specimen at three different spots, and these were then averaged for subsequent analysis.

The acquired spectra were normalized by the detector live time and evaluated in counts of photons per second (cps). Considering the area under each peak, 10 spectral lines (K-lines of Al, Si, K, Ca, Ti, Mn, Fe, Ni, and Cu, and the scattering peak Rh-Kα Compton) were selected to be used as explanatory variables, following the criteria recommended by Tavares et al. (2020).

XRF data modeling

The set comprising 101 soil samples was divided into two groups, one for calibration (with 68 samples) and the other for validation (with 33 samples) of the predictive models, procedure performed using the Kennard–Stone algorithm (Kennard and Stone, 1969) executed on the soil fertility attributes (Y-variables). Predictive models were built with multiple linear regression using the 10 XRF spectral lines as X-variables. For evaluating the effect of moisture content on the predictions, predictive models were calibrated (using the calibration set) on samples with 0% of moisture content and validated (using the validation set) on samples with moisture content of 0, 5, 10, 15, 20, and 25 wt.%. The samples were moistened with the aid of a pipette. All the calibrations and validations were performed using the Unscrambler software, version 10.5.1 (Camo AS, Oslo, Norway).

The prediction performance was evaluated through the root mean square error (RMSE) and the residual prediction deviation (RPD), the latter was calculated as the ratio between the standard deviation (SD) of the laboratory measured soil property of interest and the RMSE in the prediction.

Based on the RPD values, the prediction quality of models was classified into four classes adapted from Chang et al. (2001): poor models (RPD < 1.40), reasonable models (1.40 ≤ RPD < 2.00), good models (2.00 ≤ RPD < 3.00), and excellent models (RPD ≥ 3.00).

Results and Discussion

Laboratory Measured Soil Properties

The descriptive statistics of the fertility attributes for the calibration and validation datasets are shown in Table 1. The range and SD of soil attributes in the calibration set are close to those in the validation set, which is expected since we applied Kennard Stone method in sample split to avoid undesirable influences on the prediction accuracy that are not sensor-related (Stenberg et al., 2010).

Strong correlations exist between ex-Ca and the contents of V (r = 0.92) and ex-Mg (r = 0.84) (Table 2). These correlations suggest that if total and extractable Ca contents are correlated, indirect predictions of V and ex-Mg can occur using the Ca-Kα. Correlations of OM with the other elements ranged from 0.44 to 0.62.

Table 1. Descriptive statistics of organic matter (OM), base saturation (V) and exchangeable (ex-) Mg for the calibration and validation dataset.

	OM		**V**		**ex-Mg**	
	Cal set	Val set	Cal set	Val set	Cal set	Val set
Min	14.00	18.00	19.00	28.00	3.00	3.00
Mean	24.78	26.62	64.99	64.15	18.06	17.50
Max	37.00	35.00	92.00	91.00	54.00	47.00
SD	6.13	5.48	21.96	23.42	12.58	12.81
CV (%)	24.72	20.58	33.80	36.51	69.65	73.22

The minimum (min), maximum (max), mean, and standard deviation (SD) values of OM content were given in g dm^{-3} and, in $mmol_c$ dm^{-3}, for V and ex-Mg. The number of samples (*n*) used for the calibration (Cal) and validation (Val) sets were, respectively, 68 and 34.

Table 2. Correlation matrix of organic matter (OM), base saturation (V), exchangeable (ex-) Mg, and ex-Ca.

	OM[1]	**V**[3]	**ex-Ca**[4]	**ex-Mg**[4]
OM	1.00	0.62*	0.55*	0.44*
V		1.00	0.92*	0.84*
ex-Ca			1.00	0.93*
ex-Mg				1.00

Significant correlation at the probability level of 0.01 were indicated with an "*"; the correlations were presented on grayscale highlighting the strongest values.

Effect of moisture content on XRF data and its prediction performance

Figure 1 shows that the higher the moisture content in the soil sample, the lower is the intensity of its XRF lines. However, this behavior is inverted for the scattering peaks (Compton and Thomson scattering of Rh X-ray tube), which increase its intensity as the amount of water in the sample increases. This behavior occurs because the fluorescence lines are attenuated in the presence of water, while the scattering peaks are inversely proportional to the average atomic number of the sample, i.e., as H and O increase (present in H_2O molecule), the average atomic number of the sample decreases.

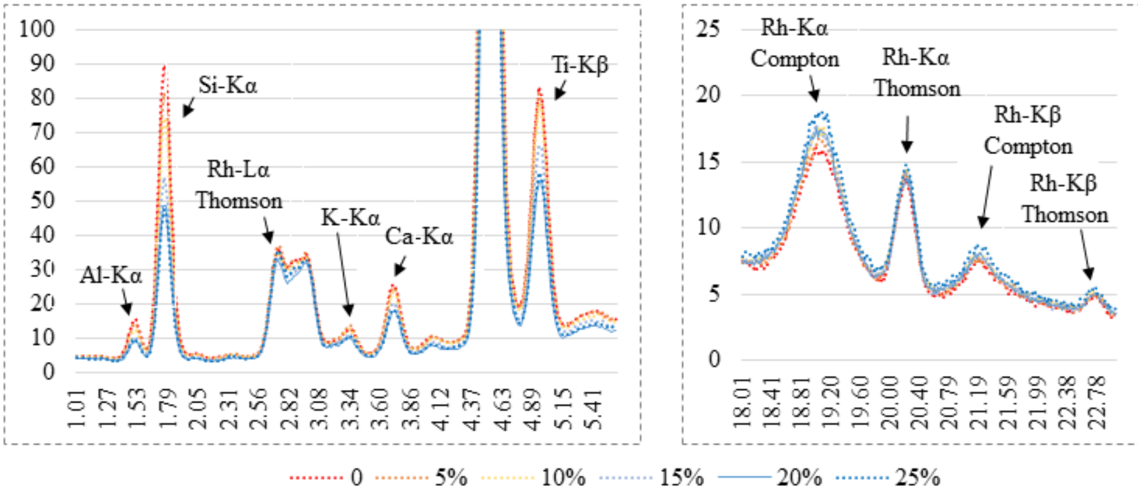

Fig 1. X-ray fluorescence emission of a dried soil sample (0%) and after increasing its gravimetric moisture content by 5, 10, 15, 20, and 25 %.

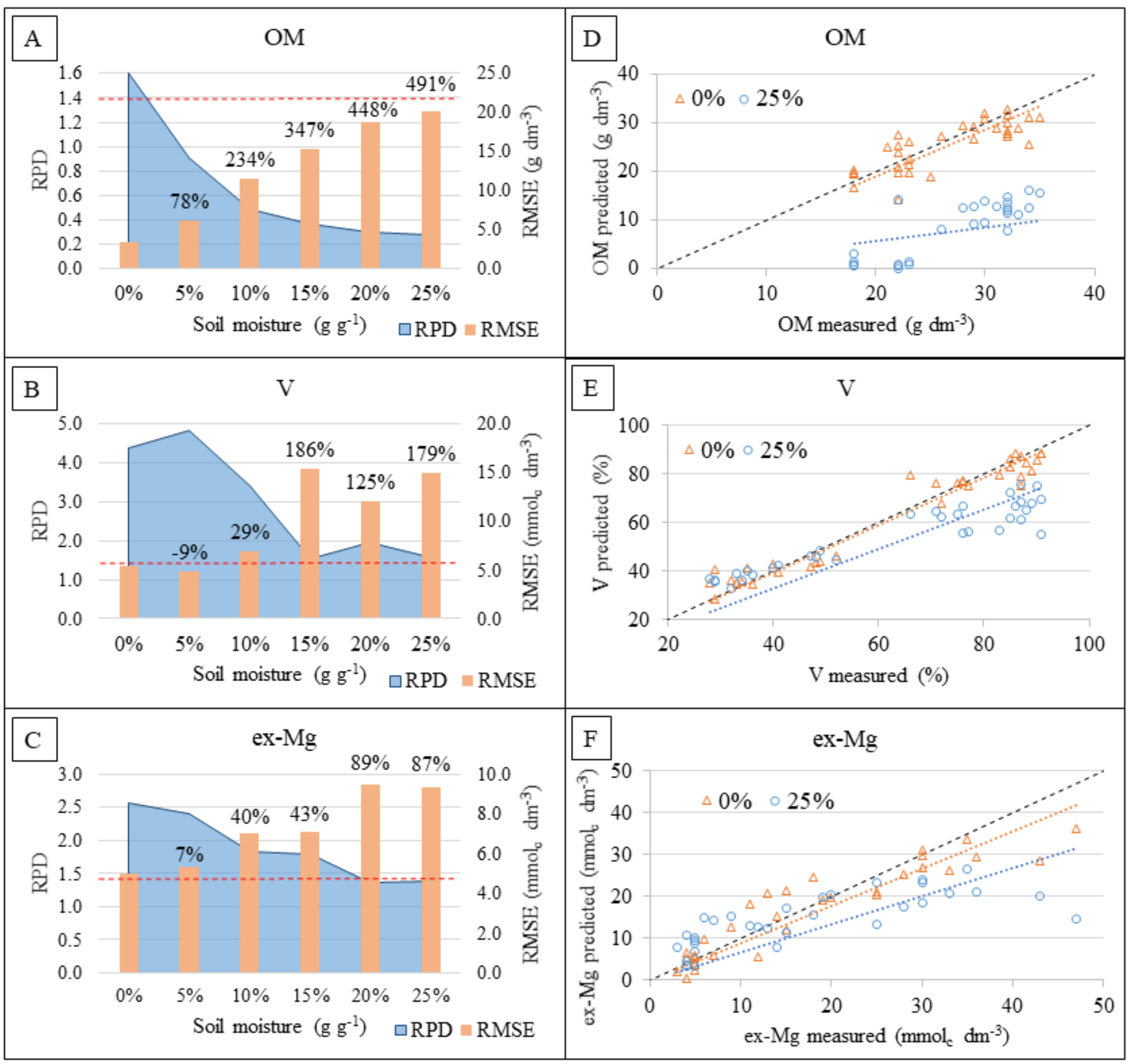

Fig 2. Effect of soil moisture increment on the performance of XRF to predict OM (A, D). V (B, E), and ex-Mg (C, F). sensors for predicting fertility attributes. The labels in graphs A, B, and C correspond to the increase in RMSE (in percentage) compared to the RMSE obtained on dry samples (0% of moisture content). The red dashed line indicates a RPD of 1.4, values below this threshold indicate poor performance.

Regarding the prediction of fertility attributes using the XRF sensor, it is evident the reduction of its predictive performance as the moisture content increases (Fig. 2), which occurred for all studied soil attributes. The prediction error of the XRF sensor increased between 29 and 234% in the second increment of water (samples with 10% of moisture content), reaching an increase between 87 and 491% in samples with 25% of moisture content. OM was the attribute that most lost performance when increasing the water content, while the V was the one that least lost performance. Despite the loss of performance of the XRF sensor when increasing the soil moisture content, our results shown that it is possible to reach satisfactory prediction performances (RPD ≥ 1.40) for V, at all moisture conditions, and for ex-Mg up to 15% of moisture content (Fig. 2). The emission lines that most contributed to each predictive model are shown in Figure 3.

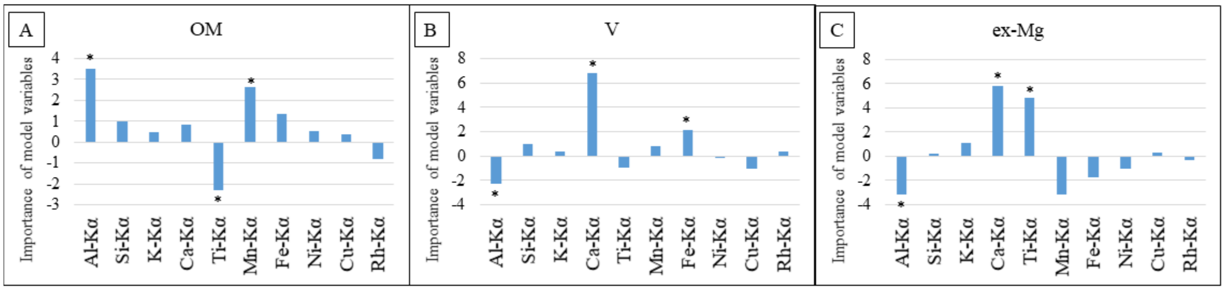

Fig 3. Importance of variables for predictive models of organic matter (OM), base saturation (V) and exchangeable (ex-) Mg.

Unlike laboratory measurements that are mainly conducted on dry and sieved samples, sensors applied in field conditions need to deal with external factors (*e.g.*, soil moisture, soil roughness, etc) that influence sensors' output (Horta et al., 2015, Mouazen and Al-Asadi, 2018). Soil moisture is one of the most studied external factor due to its marked influence on sensor's performance (Angelopoulou et al., 2020). Regarding the moisture effect on XRF sensor's performance for fertility analysis, our results showed that predictive models calibrated on dry samples can be satisfactorily replicated on wet samples, especially for some specific attributes (e.g., V in our case). Nevertheless, it was observed that indeed there is a loss of performance when increasing the water content in the soil. So, in cases where it is necessary to maintain the prediction accuracy, methods adopted to minimize external effects such as external parameter orthogonalization (EPO) (Roger et al., 2003) and direct standardization method (Wang et al., 1995) should be considered. Although the abovementioned methods have shown promising results for vis-NIR sensors providing moisture-insensitive predictions of soil attributes (Minasny et al., 2011; Kuang and Mouazen et al., 2013; Nawar et al., 2020), they have not yet been explored for XRF, which should be encouraged in future research. In addition, studies applying XRF sensors directly in the field are also necessary in order to consider the influence of other factors, such as soil roughness, ambient temperature, residues (*e.g.*, stones and straw), and some movement during spectral acquisition, which can also interfere *in situ* measurements (Angelopoulou et al., 2020).

Conclusion

The XRF sensor gradually reduced its predictive performance by increasing the water level (from 0 to 25 wt.%) in the soil. Despite this, our results shown that it is possible to reach satisfactory prediction performances (RPD ≥ 1.40) for base saturation (V), at all evaluated moisture conditions, and for exchangeable (ex-) Mg, up to 15% of moisture content. Unlike the other attributes, organic matter (OM) predictions were not possible on wet soils when using predictive models calibrated on dry soils.

The observed results emphasize the potential of XRF for *in situ* analysis of soil fertility attributes, since with a reduced scanning time (e.g., 4 s) it is possible to obtain satisfactory prediction performances in wet samples. Furthermore, our results encourage future research to find the best method for mitigating the effect of soil moisture content in XRF spectra.

Acknowledgements

We acknowledge the financial support provided by São Paulo Research Foundation (FAPESP) to T.R.T. related to the grant number 2020/16670-9.

References

Adamchuk, V. I., Lund, E. D., Reed, T. M., & Ferguson, R. B. (2007). Evaluation of an on-the-go technology for soil pH mapping. Precision Agriculture, 8(3), 139-149.

Angelopoulou, T., Balafoutis, A., Zalidis, G., & Bochtis, D. (2020). From laboratory to proximal sensing spectroscopy for soil organic carbon estimation—A review. Sustainability, 12(2), 443.

Chang, C. W., Laird, D. A., Mausbach, M. J., & Hurburgh, C. R. (2001). Near-infrared reflectance spectroscopy–principal components regression analyses of soil properties. Soil Science Society of America Journal, 65(2), 480-490.

Ge, L., Lai, W., & Lin, Y. (2005). Influence of and correction for moisture in rocks, soils and sediments on in situ XRF analysis. X-Ray Spectrometry: An International Journal, 34(1), 28-34.

Horta, A., Malone, B., Stockmann, U., Minasny, B., Bishop, T. F. A., McBratney, A. B., ... & Pozza, L. (2015). Potential of integrated field spectroscopy and spatial analysis for enhanced assessment of soil contamination: a prospective review. Geoderma, 241, 180-209.

Khosla, R., & Alley, M. M. (1999). Soil-specific nitrogen management on mid-Atlantic coastal plain soils. Better Crops, 83(3), 6-7.

Kennard, R. W., & Stone, L. A. (1969). Computer aided design of experiments. Technometrics, 11(1), 137-148.

Kuang, B., & Mouazen, A. M. (2013). Non-biased prediction of soil organic carbon and total nitrogen with vis–NIR spectroscopy, as affected by soil moisture content and texture. Biosystems Engineering, 114(3), 249-258.

Lima, T. M., Weindorf, D. C., Curi, N., Guilherme, L. R., Lana, R. M., & Ribeiro, B. T. (2019). Elemental analysis of Cerrado agricultural soils via portable X-ray fluorescence spectrometry: Inferences for soil fertility assessment. Geoderma, 353, 264-272.

Minasny, B., McBratney, A. B., Bellon-Maurel, V., Roger, J. M., Gobrecht, A., Ferrand, L., & Joalland, S. (2011). Removing the effect of soil moisture from NIR diffuse reflectance spectra for the prediction of soil organic carbon. Geoderma, 167, 118-124.

Mouazen, A. M., & Al-Asadi, R. A. (2018). Influence of soil moisture content on assessment of bulk density with combined frequency domain reflectometry and visible and near infrared spectroscopy under semi field conditions. Soil and Tillage Research, 176, 95-103.

Molin, J. P., & Tavares, T. R. (2019). Sensor systems for mapping soil fertility attributes: Challenges, advances, and perspectives in brazilian tropical soils. Engenharia Agrícola, 39, 126-147.

Nawar, S., Delbecque, N., Declercq, Y., De Smedt, P., Finke, P., Verdoodt, A., ... & Mouazen, A. M. (2019). Can spectral analyses improve measurement of key soil fertility parameters with X-ray fluorescence spectrometry?. Geoderma, 350, 29-39..

Nawar, S., Abdul Munnaf, M., & Mouazen, A. M. (2020). Machine learning based on-line prediction of soil organic carbon after removal of soil moisture effect. Remote Sensing, 12(8), 1308.

O'rourke, S. M., Stockmann, U., Holden, N. M., McBratney, A. B., & Minasny, B. (2016). An assessment of model averaging to improve predictive power of portable vis-NIR and XRF for the determination of agronomic soil properties. Geoderma, 279, 31-44.

Roger, J. M., Chauchard, F., & Bellon-Maurel, V. (2003). EPO–PLS external parameter orthogonalisation of PLS application to temperature-independent measurement of sugar content of intact fruits. Chemometrics and Intelligent Laboratory Systems, 66(2), 191-204.

Stenberg, B., Rossel, R. A. V., Mouazen, A. M., & Wetterlind, J. (2010). Visible and near infrared spectroscopy in soil science. Advances in agronomy, 107, 163-215.

Stockmann, U., Cattle, S. R., Minasny, B., & McBratney, A. B. (2016). Utilizing portable X-ray fluorescence spectrometry for in-field investigation of pedogenesis. Catena, 139, 220-231.

Tavares, T. R., Molin, J. P., Nunes, L. C., Alves, E. E. N., Melquiades, F. L., de Carvalho, H. W. P., & Mouazen, A. M. (2020). Effect of X-ray tube configuration on measurement of key soil fertility attributes with XRF. Remote Sensing, 12(6), 963.

Tavares, T. R., Nunes, L. C., Alves, E. E. N., Almeida, E. D., Maldaner, L. F., Krug, F. J., ... & Molin, J. P. (2019). Simplifying sample preparation for soil fertility analysis by X-ray fluorescence spectrometry. Sensors, 19(23), 5066.

Viscarra Rossel, R., Adamchuk, V. I., Sudduth, K. A., McKenzie, N. J., & Lobsey, C. (2011). Proximal soil sensing: An effective approach for soil measurements in space and time. Advances in Agronomy, 113, 243-291.

Wang, Z., Dean, T., & Kowalski, B. R. (1995). Additive background correction in multivariate instrument standardization. Analytical Chemistry, 67(14), 2379-2385.

Weindorf, D. C., Zhu, Y., McDaniel, P., Valerio, M., Lynn, L., Michaelson, G., ... & Ping, C. L. (2012). Characterizing soils via portable x-ray fluorescence spectrometer: 2. Spodic and Albic horizons. Geoderma, 189, 268-277.

Weindorf, D. C., & Chakraborty, S. (2020). Portable X-ray fluorescence spectrometry analysis of soils. Soil Science Society of America Journal, 84(5), 1384-1392.